Indian Journal of Chemistry
Vol. 62, August 2023, pp. 808-815
DOI: 10.56042/ijc.v62i8.198

Quantum chemical and third order nonlinear optical investigation of (E)-1-(1*H*-imidazol-1-yl)-3-(1*H*-indol-2-yl)prop-2-en-1-one

G Arjunan[a], R Karunathan[b], R Raj Muhamed[c] & V Sathyanarayanamoorthi*[a]

[a] Department of Physics, PSG College of Arts And Science, Coimbatore 641 014, India
[b] Department of Physics, Dr. NGP Arts and Science College, Coimbatore 641 035, India
[c] Department of Physics, Jamal Mohamed College, Trichy 620 020, India

E-mail: sathyanarayanamoorthi@psgcas.ac.in

Received 29 March 2023; accepted(revised) 17 July 2023

In this study, quantum chemical and spectroscopic techniques were used to investigate (E)-1-(1H-imidazol-1-yl) and (3-(1H-indol-2-yl))prop-2-en-1-one. Density functional theory simulations at the B3LYP/6-31++G(d,p) level of theory were performed to analyse the geometrical characteristics, NLO activity, and frontier molecular orbitals of synthesised substances. Frontier molecular orbitals (FMOs) analysis was done to determine the kinetic stability of the synthesised compound. The dipole moment and initial hyperpolarizabilities of the investigated compounds demonstrate their suitability as potential nonlinear optical materials. Moreover, molecular structure, vibrational assignments, ^{1}H and ^{13}C NMR chemical shift values were also taken and analysed for the titled compound.

Keywords: Quantum chemical, Spectroscopic, Nonlinear, HOMO-LUMO, NMR

Chemicals from the flavonoid family which are known as chalcones, can be produced synthetically or naturally [1]. Two aromatic rings are linked by a three-carbon, α,β-unsaturated carbonyl system to form open-chain flavonoids. Chalcones have been associated with a wide range of pharmacological actions, such as antimalarial, anti-tubercular, and anti-leishmanial properties, as well as anti-cancer, anti-bacterial, and anti-inflammatory properties[2–11]. Numerous chalcones have been reported to have strong anti-malarial activity[12]. Chalcones are advantageous as organic nonlinear optical materials (NLO) because of their second-harmonic generation (SHG) conversion efficiency[13]. Because of their potent molecular hyperpolarizabilities, organic materials display a variety of significant non-linear optical properties. Numerous important chemical and physical properties of biological and chemical systems can be anticipated using computational techniques from the very beginning[14,15]. The density functional theory (DFT) method is a popular high-fidelity (HF) method for computing the structural characteristics, vibrational frequencies, and energies of molecules[16], as well as for its efficacy and accuracy in determining molecular properties[17,18]. Recently, the *ab initio* community has accepted this method. Imidazole is one of the highly polar five-membered heterocyclic rings that include nitrogen. It will dissolve in water. The six electrons required for aromaticity are provided by the solitary pair of electrons that the nitrogen linked to the hydrogen has. The hydrogen atom can be located on either of the two nitrogen atoms in imidazole because of its resonance structures[19]. Numerous studies have already shown that imidazoles and their modified derivatives have a wide range of biological applications. In-depth molecular studies are being done on the origin and mechanism of the chemicals' biological activity[20]. Imidazoles and their derivatives, in particular, have anti-parasitic, anti-tumoral, antihistaminic, antihypertensive, anti-cancer[21-23], antibacterial, and antifungal properties[24-25]. In this article, we describe how to make (E)-1-(1H-imidazol-1-yl)-3-(1H-indol-2-yl)prop-2-en-1-one with spectroscopic properties, in continuation of our current work on the creation of imidazole analogues as structural and spectroscopic properties consideration. In order to do this, fluorophenyl groups were combined with imidazole as spacers in a single framework.

In order to understand the structure-activity relationship, the title chemical has been examined

using density functional theory (DFT). With the aid of FT-IR, NMR, and single-crystal X-ray diffraction, the structure of the chemical was determined. The HF and DFT/B3LYP methods in the 6-311++G(d,p) basis set were also used to estimate the molecule's structural and spectroscopic properties in the gas phase. In this article, the topic chemical's spectroscopic and theoretical research findings are presented.

Methods and Materials

Synthesis of (E)-1-(1*H*-imidazol-1-yl)-3-(1*H*-indol-2-yl)prop-2-en-1-one

Equimolar quantity of indole–2–carboxaldehyde (0.01 mol) and 1-acetyl imidazole (0.01 mol) were dissolved in 20 mL of ethanol in a 150 mL round bottomed flask. The reaction mixture was magnetically stirred for 3h in ice-cold condition and during stirring 10 mL of 10% sodium hydroxide solution was added drop wise. A flocculants precipitate was formed. The precipitate was filtered and washed with cold water. The solid obtained was purified by column chromatography using silica gel 60-120 mesh and n-hexane: acetone (7:3 v/v) as elevate.

Characterization techniques

In order to confirm the chemical structure, the ^{1}H NMR and ^{13}C NMR spectra were recorded by employing a Bruker 500 MHz spectrometer in deuterated solvents using DMSO (dimethyl sulfoxide-d_6) as the internal reference standard. In the present work, the functional group was identified using a JASCO-FT-IR 5300 infrared spectrometer in the frequency region of 400-4000 cm^{-1} by employing the KBr pellet technique with a spectral resolution of 4.0 cm^{-1}. Optical absorption spectra were recorded at room temperature using a Perkin-Elmer Lambda 35 Spectrophotometer in the wavelength region of 200-850 nm. The theoretical quantum chemical studies were performed at DFT [B3LYP (Becke's three-parameter (B3) exchange in conjunction with the Lee–Yang-Parr's (LYP) correlation functional] method with B3LYP/6-31++G (d,p) basis set using Gaussian 09 program[26-28]. The molecular structure was optimized from crystallographic information file (CIF) as source, and all calculations were computed by this optimized structure only. GaussView 5.0 visualization program has been employed to shape HOMO and LUMO orbitals[29].

Results and Discussion

Absorption spectrum

The UV-visible spectrum gives limited information about the structure of the molecule because the absorption of UV and visible light involves the promotion of the electron from the ground state to higher energy states. The electronic absorption spectrum of the title compound is depicted in Fig. 1. The absorption peak at 315 nm is attributed to the charge transfer transition between the donor and acceptor of the system. The absorption band raised due to the promotion of an electron from the highest occupied orbital to the lowest unoccupied molecular orbital confirms the formation of a charge transfer molecular complex. The spectrum indicates that there is no significant absorption in the visible and near infrared regions.

NMR Spectral Analysis

Nuclear magnetic resonance (NMR) is a versatile technique employed to identify the molecular structure. The ^{1}H NMR and ^{13}C NMR spectra of the title molecule were recorded using DMSO as solvent. The recorded ^{1}H and ^{13}C NMR spectra are shown in Table 1, Fig. 2a and b, respectively. In the ^{1}H NMR spectrum, the appearance of 7 distinct proton signals confirms the formation of the crystal. The singlet at δ 12.19 ppm is due to the nitrogen proton of the Indole moiety. The peak centered at δ 9.99 ppm is assigned to the CH of aldehyde moiety. The peak centered at δ 8.31 ppm owes to the CH proton of indole–2–carboxaldehyde moiety. The CH aromatic proton of Indole moiety appears at δ 8.16 ppm. The CH protons of acetyl imidazole moiety appear at δ 7.29 ppm. The signal observed at δ 3.48 ppm represents the protons due to acetyl moiety of the molecule. The aromatic and aliphatic proton of the molecule observed at δ

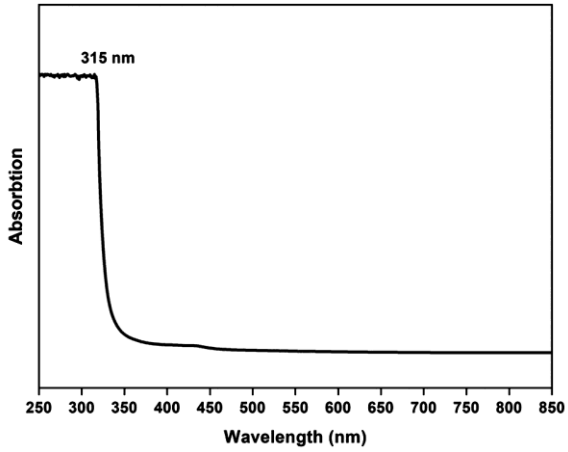

Fig. 1 — Optical absorption spectrum.

Table 1 — The recorded ^{1}H and ^{13}C NMR spectral values

Peak	Description (^{1}H NMR)	δ (ppm)
1	N proton of Indole Moiety	12.19
2	CH of aldehyde moiety	9.99
3	CH of indole–2–carboxaldehyde moiety	8.31
4	CH aromatic proton of Indole moiety	8.16
5	CH proton of acetyl imidazole	7.29
6	CH Proton of acetyl portion of molecule	3.48
7	aromatic and aliphatic proton of the molecule	2.52
	Description (^{13}C NMR)	δ (ppm)
8	Carbonyl carbon of C=O moiety	185
9	Carbon in the imidazole moiety	138
10	Carbon in the indole moiety	123
11	Carbon in the aromatic ring	112
12	Aliphatic carbons	40

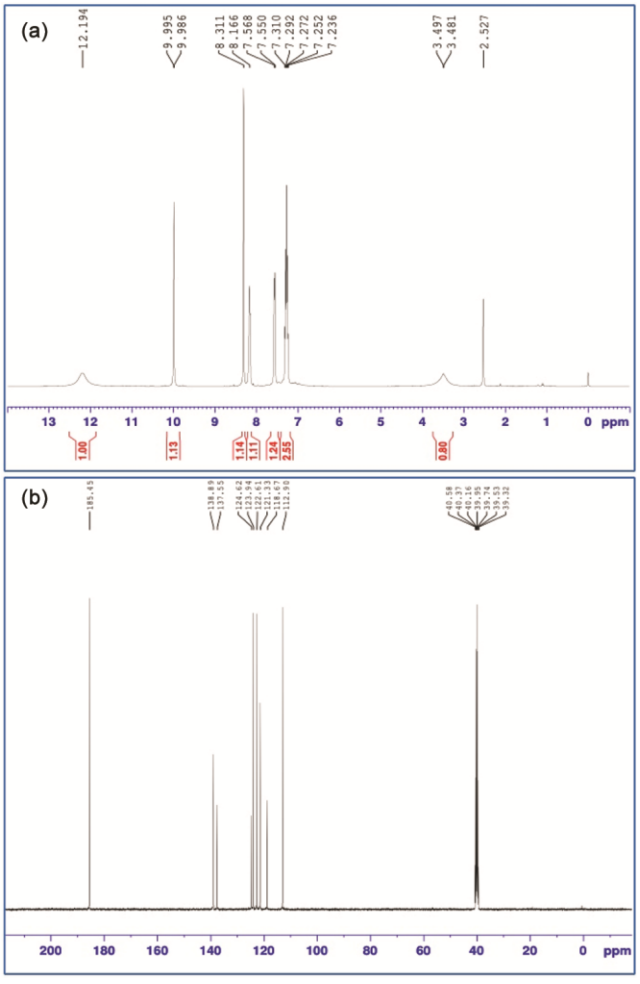

Fig. 2 — (a) ^{1}H and (b) ^{13}C NMR spectrum of the compound.

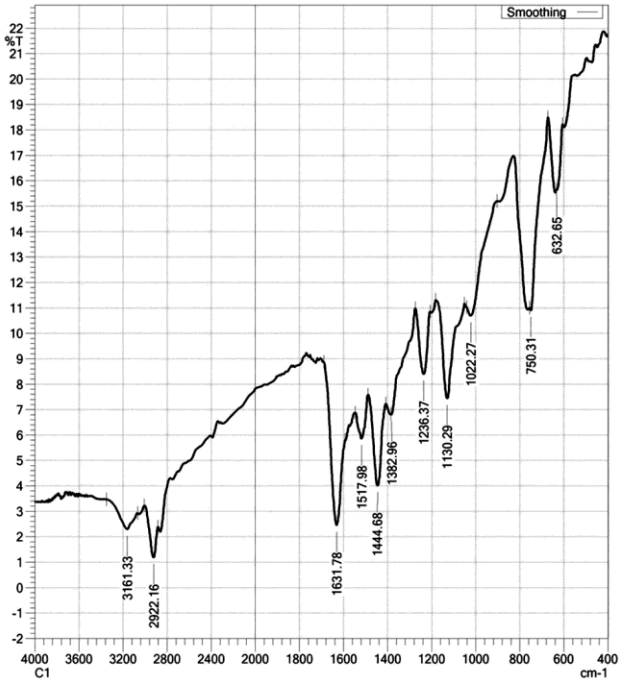

Fig. 3 — FTIR spetrum.

2.52 ppm. The appearance of carbon signals in the spectrum explicitly confirms the molecular structure of the complex. The carbon signal at δ 185 ppm owes to the highly deshielded carboxyl carbon atoms of the molecule. The carbon signal at δ 138 ppm is attributed to the carbon of the imidazole moiety. The carbon signal at δ 123 ppm is attributed to the carbon of the indole moiety. The carbon signal at δ 112 ppm is due to the carbon of the aromatic ring in the molecule. The signal at 40 ppm owes to the aliphatic carbon of the molecule. Thus, the molecular structure of the complex stands confirmed from the ^{1}H and ^{13}C NMR spectral data.

FTIR analysis

The well assignment of the bands, observed in the vibrational spectra, is an indispensable step for solving the structural problems of any molecule. The IR spectrum of title molecule in the region 4000–400 cm^{-1} is shown graphically in Fig. 3. The details of the various vibrations and their assignments are discussed in the subsequent sections. The broad absorption band appearing at 3161 cm^{-1} is due to aromatic C-H stretching vibration of the molecule. The sharp absorption band at 2922 cm^{-1} is due to the aliphatic C-H stretching vibration. The C=C stretching vibration is observed at 1631 cm^{-1}. The C=C stretching vibration of indole moiety appears at 1517

cm^{-1}. The band at 1444 cm^{-1} is due to the C-N stretching vibration of imidazole. For indole moiety, the C-N stretching vibration is observed at 1382 cm^{-1}. The C-H stretching vibration of molecule is observed at 1236 cm^{-1}. The C-H stretching vibration of Indole and imidazole moiety is observed at 1130 cm^{-1} and 1022 cm^{-1}. The C-H wagging vibration is observed at 750 cm^{-1}. The peak at 632 cm^{-1} is assigned to benzene ring vibration.

Raman Spectroscopy

The title molecule was also subjected to Raman spectroscopy. The observed frequency for the molecule is shown in the Fig. 4. The peak observed at 3114 cm^{-1} is attributed to aromatic C-H stretching vibration of the molecule. The band at 3063 cm^{-1} is attributed to the aliphatic C-H stretching vibration. The band at 1633 cm^{-1} is due to C=C stretching vibration. The C=C stretching vibration of indole moiety appears at 1522 cm^{-1} in the raman spectrum. The band at 1395 cm^{-1} is assigned to the C-N stretching vibration of imidazole. The C-N stretching vibration is observed at 1336 cm^{-1} for indole moiety. The raman C-H scissoring vibration of molecule is observed at 1243 cm^{-1}. The C-H scissoring vibration of Indole and imidazole moeity is observed at 1150 cm^{-1} and 1007 cm^{-1}. The peak at 789 cm^{-1} is assigned to C-H wagging vibration. The benzene ring vibration is observed at 641 cm^{-1}.

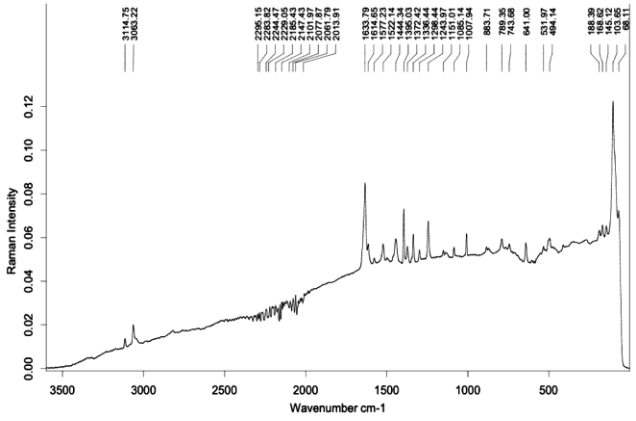

Fig. 4 — FT-Raman spectra of the title compund.

Optimized Geometry

The molecular structure is optimized by DFT/B3LYP method with 6-31++G (d,p) basis set. Atom numbering scheme adopted for the molecule and the same molecule were positioned in the Cartesian axis for optimization of the structure. The optimized geometry of the title compound is shown in Fig. 5. The title molecule has two Indole group and imidazole group systems. The indole group and imidazole groups are bridged by propene group. The calculated bond length and bond angle are given in Table 2. The four types of bond lengths (C-C, C-N, C-H and C-O) presented in title molecule and these values are listed in Table 2. The bond length of C-N found to be C14-N18=1.4025Å, C16-N15 = 1.4059, C13-1.3818. It is observed that the bond length of C1=O4 is 1.2456 The other standard bond lengths and bond angles are listed in Table 2 and are in good agreement to similar structure with very small deviation. The same optimized structure is used for further DFT calculations for more understanding the structural properties.

Analysis of Frontier Molecular Orbitals

The highest occupied molecular orbitals (HOMOs) and the lowest-lying unoccupied molecular orbitals (LUMOs) are named as Frontier Molecular Orbitals (FMOs) because they lie at the outermost boundaries of the electrons of compound. The frontier orbital gap helps characterize the chemical reactivity and the kinetic stability of the molecule. A molecule with a small frontier orbital gap is termed as soft molecule and is generally associated with high chemical reactivity and low kinetic stability[30]. In addition, the

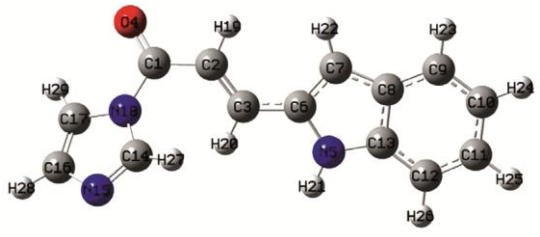

Fig. 5 — Optimized geometry.

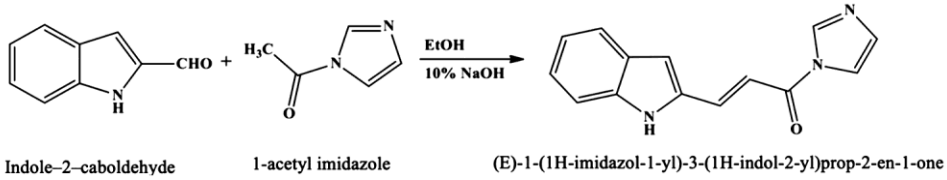

Scheme 1 — Reaction scheme of the synthesized compound.

Table 2 — Selected Bond length and bond angle of the title compound.

Bond Length (Å)		Bond Angle (°)	
C2-C1	1.461857		
C2-C3	1.35817	C1-C2-C3	125.909
C1-04	1.24568	C2-C1-O4	122.0252
C3-N5	2.468233	C3-C3-N5	154.9606
C6-N5	1.405342	C3-N5-C6	30.17604
C6-C7	1.391861	N5-C6-C7	107.9072
C7-C8	1.429001	C6-C7-C8	107.9651
C8-C9	1.41184	C8-C9-C7	133.8733
C9-C10	1.389068	C8-C9-C10	118.9033
C10-C11	1.417575	C9-C10-C11	121.1287
C11-C12	1.391789	C10-C11-C12	121.4591
C13-N5	1.381871	C3-N5-C13	139.994
C14-C1	2.561494	O4-C1-C14	140.2338
C14-N15	1.320287	C1-C14-N15	136.6203
C16-N15	1.405924	C14-N15-C16	105.8511
C16-C17	1.369305	N15-C16-C17	110.4718
C17-N18	1.402168	C16-C17-N18	106.0032
C2-H19	1.084933	C1-C2-H19	113.0565
C3-H20	1.088051	C2-C3-H20	118.6836
N5-H21	1.006797	C3-N5-H21	94.54906
C7-H22	1.07928	C6-C7-H22	125.615
C9-H23	1.08521	C8-C9-H23	120.3657
C10-H24	1.084924	C9-C10-H24	119.7916
C11-H25	1.085095	C10-C11-H25	119.1968
C12-H26	1.085146	C11-C12-H26	121.1112
C14-H27	1.075256	C1-C14-H27	97.26542
C16-H28	1.076733	N15-C16-H28	120.8604
C17-H29	1.075307	C16-C17-H29	133.1141

FMOs are important in determining the ability of a molecule to absorb light. The FMOs play an important role in the optical and electric properties, as well as in quantum chemistry and UV–vis spectra. HOMO, LUMO energy characterizes the ability of electron accepting. In dealing with interacting molecular orbitals, the two that interact are generally the highest energy occupied molecular orbital (HOMO) and lowest unoccupied molecular orbital (LUMO) of the compound. These orbitals are a pair of orbitals in the compound, which allows them to interact more strongly. In order to evaluate the energetic behaviour of the title compound, the calculations were carried out in gas phase. The calculated energy values of HOMO and LUMO in the gas phase are 5.9636 eV and 2.4857 eV, respectively, and the frontier orbital energy gap value is 3.4788 eV. HOMO and LUMO energies and surfaces can be seen in Fig. 6. The narrow energy gap between HOMO and LUMO facilitates intramolecular charge transfer which makes the material to be NLO active.

Moreover, the energy band gap value helps us to identify the chemical reactivity and kinetic stability of a molecule. A small band gap energy of the molecule

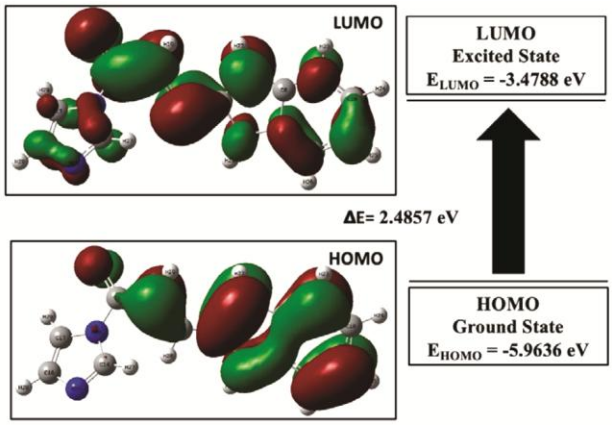

Fig. 6 — Frontier molecular orbital analysis.

is generally related to high chemical reactivity and low kinetic stability. The ionisation energy (I) and electron affinity (A) are of great importance in the determination of biochemical pathways for electron transfer, photosynthesis, oxidative phosphorylation, and oxidative stress. The Ionisation energy is directly proportional to the electrochemical oxidation potentials of the compounds. The electron affinity gives an idea about the stability of free radicals and anions. The ionisation energy and electron affinity can be expressed through HOMO and LUMO orbital energies by Koopmans' theorem[31] as, $I=-E_{HOMO}$ and $A=-E_{LUMO.}$ From the value of ionization energy and electron affinity, Mulliken electronegativity (χ) can be calculated from the equation $\chi = (I+A)/2$. The chemical potential (μ) is the negative value of the electronegativity. Softness (S) is a property of the molecule that measures the extent of chemical reactivity. It is the reciprocal of hardness ($S= 1/2\eta$). The hardness is calculated using the expression $\eta = (I-A)/2$[32]. Parr *et al*., have proposed the global electrophilicity power of a system as, $\omega = \mu^2 / 2\eta$[33]. This index measures the stabilisation in energy when the system acquires an additional electronic charge from the environment. The values of electronegativity, chemical hardness, softness, and electrophilicity index of the title molecule are 4.7212 eV, 1.2458 eV, 0.4023 eV, and 3.789 eV in the gas phase, respectively.

Hyperpolarizability study

The interactions of electromagnetic fields in various materials produce the nonlinear optical (NLO) effects by altering the phase, frequency, amplitude or other propagation characteristics from the incident

fields[34]. The hyperpolarizability and non-linear optical properties of an isolated molecule of potential NLO materials are considered as an extensive tool of research in molecular spectroscopy. To design the novel NLO materials, the theoretical investigation plays a key role in understanding the structure–property relationship. As the basis set of the density functional calculation becomes larger, one can expect a better description of the compound and, accordingly more accurate results. In view of these points, B3LYP/6-31G++G(d,p) method has been used to study the hyperpolarizability of the crystal. The complete equations for calculating the magnitude of the total static dipole moment (μ), mean polarizability (α), anisotropy of polarizability (Δα) and first order hyperpolarizability (β) from Gaussian output are given below:

$$\mu = \sqrt{(\mu_x{}^2 + \mu_x{}^2 + \mu_x{}^2)}$$

$$\alpha = \frac{(\alpha_{xx} + \alpha_{yy} + \alpha_{zz})}{3}$$

$$\Delta\alpha = \sqrt{2}\left[(\alpha_{xx} - \alpha_{yy})^2 + (\alpha_{yy} - \alpha_{zz})^2 + (\alpha_{zz} - \alpha xx2 + 6\alpha xx212\right.$$

$$\beta = \left[(\beta_{xxx} + \beta_{xyy} + \beta_{xzz})^2 + (\beta_{yyy} + \beta_{yzz} + \beta_{yxx})^2 + (\beta_{zzz} + \beta_{zxx} + \beta_{zyy})^2\right]^{1/2}$$

The polarizabilities and hyperpolarizability are reported in terms of atomic units (a.u) and the calculated values have been converted by using 1 a.u. = 0.1482×10^{-24} esu for α and 1 a.u. = 8.6393×10^{-33} cm^5/esu for β. In the calculations, the values of the calculated dipole moment (μ), mean polarizability (α) and anisotropy of polarizability (Δα) are 6.8815 Debye, 1.11 Å esu, 1.412 Å esu.

Mulliken Atomic Charge

A major function for the application of quantum chemical calculation to a molecular system was the Mulliken calculation of atomic charges. Atomic charges depend on the dipole moment, molecular polarisation, electronic structure, and many of molecular system characteristics. The charge distributions over the atoms advocate the creation, in the molecule, of donor and acceptor pairs. Fig. 7 shows the calculated (E)-1-(1H-imidazol-1-yl)-3-(1H-indol-2-yl)prop-2-en-1-one Mulliken load distribution structure. There are more negative charges for oxygen and Nitrogen atoms, while the positive charge is present for all hydrogen atoms. Furthermore, Mulliken atomic charges also show that the nitrogen atoms have negative atomic charges in the molecule. The atomic charge variations of hydrogen atoms are formed by hydrogen bonding. The total of the atomic charge of all atoms, however, retains neutrality with regard to charge. Mulliken population analysis is a useful way for interpreting and predicting the reagent behaviours of a wide range of chemical systems for both electrophilicity and nuclear reactions to take into account the differences in charges of atoms within Mulliken population methodology.

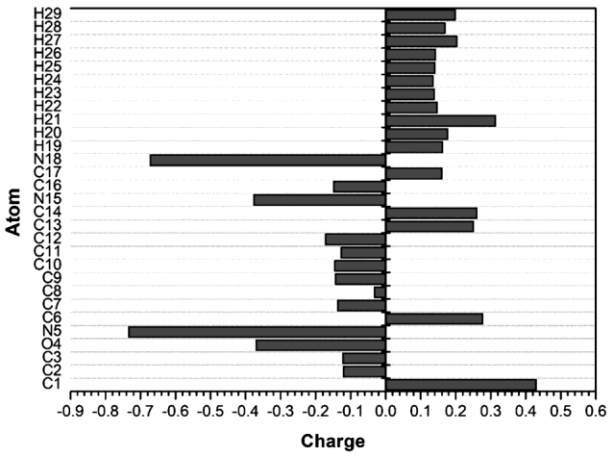

Fig. 7 — Mulliken atomic charge analysis.

Z-Scan Studies

Z-scan technique is common technique for measuring both the non-linear (n_2) and the non-linear ($\chi^{(3)}$)[35] refractive index immediately. The sample was moved through the axial direction through a focal area (-Z to + Z) which is the direction of laser beam propagation. The intensity dependent absorption of the material was measured when the sample was moved through the focus and without placing the open aperture on the detector. By monitoring the transformation through a small aperture at the far field position (closed aperture), the amplitude of the phase shift is measured carefully. The open and closed aperture measurements of the standard transmission (T) are shown in Fig. 8a and 8b. From the following relation, $\chi^{(3)}$ is calculated,

$$\left|\chi^{(3)}\right| = [(Re\chi^{(3)})^2 + (Im\chi^{(3)})^2]^{\frac{1}{2}}$$

The estimated nonlinear refractive index (n_2), nonlinear absorption coefficient and third order susceptibility values of the molecule was 7.3427×10^{-8} cm^2/W, 0.00028 cm/W and 2.63×10^{-7} esu indicates

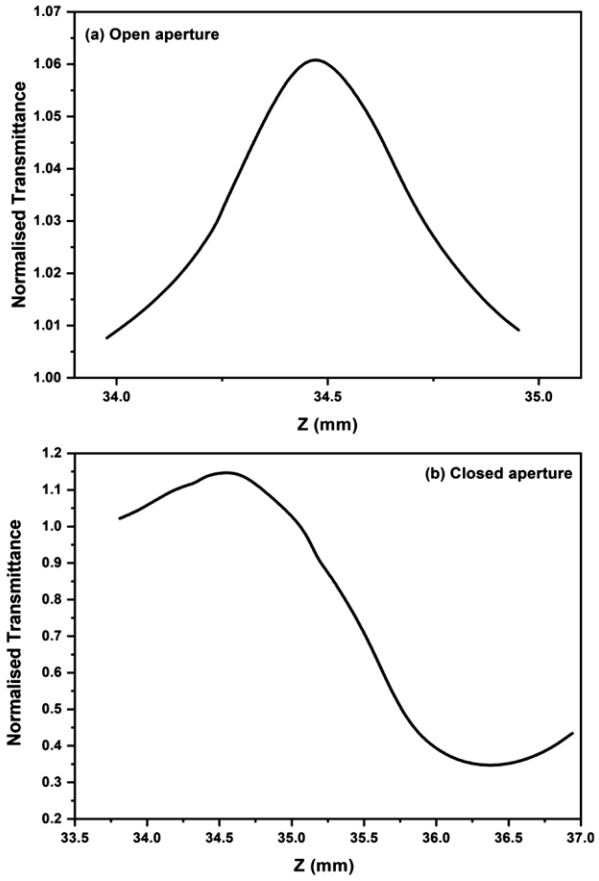

Fig. 8 — (a) Open and (b) closed aperture spectrum of Z-scan measurements.

Table 3 — Third order nonlinear optical parameters

Laser beam wave length (λ) = 632.8nm
Laser Power (P) = 35 mW
Lens focal Length (f) = 24 cm
Optical path distance (Z) = 175 cm
Effective thickness (L_{eff}) = 3 mm
Aperture radius of detector for closed (r_a) = 4 mm
Aperture radius of detector for open (r_a) = 30 mm
Incident intensity at the focus (Z = 0) = 2mW/cm^2
Nonlinear refractive index (n_2) = 7.3427×10^{-8} cm^2/W
Nonlinear absorption coefficient (β) = 0.00028 cm/W
The third-order nonlinear susceptibility ($\chi^{(3)}$) = 2.63 × 10^{-7} esu

that the material reveals a positive refractive index (Table 3). It leads to self-focused nature and displays a process of two-photon absorbance. This is one of the most important parameters for optical limits.

Conclusion

In this study, a combined experimental and theoretical investigation on E)-1-(1H-imidazol-1-yl) and (3-(1H-indol-2-yl)prop-2-en-1-one has been performed. The ^{1}H and ^{13}C NMR studies confirm the structure of the compound. FTIR and FT-Raman measurements reveal the presence of various functional groups. Absence of absorption in the visible region makes the crystal suitable for optical applications. HOMO-LUMO and Mulliken studies confirm the charge transfer and distribution of charge in the molecules. Theoretical first hyperpolarizability and experimental Z-scan studies suggest the suitability of the title compound for nonlinear optical applications.

References

1 Carlo G D, Mascolo N, Izzo A A & Capasso F, *Life Sciences*, 65 (1999) 337.
2 Go M L, Wu X & Liu X L, *Curr Med Chem*, 12 (2005) 483.
3 Hsieh H K, Tsao L T, Wang J P & Lin C N, *J Pharm Pharmacol*, 52 (2000) 163.
4 Viana G S B, Bandeira M A M & Matos F J A, *Phytomedicine*, 10 (2003) 189.
5 Epifano F, Genovese S, Menghini L & Curini M, *Phytochemistry*, 68 (2007) 939.
6 Onyilagha J C, Malhotra B, Elder M, French C J & Towers G N, *Canadian J Plant Path*, 19 (1997) 133.
7 Sivakumar P M, Priya S & Doble M, *Chem Bio Drug Des*, 73 (2009) 403.
8 Sivakumar P M, Babu S K G & Mukesh D, *Chem Pharm Bull*, 55 (2007) 44.
9 Satyanarayana M, Tiwari P, Tripathi B K, Srivastava A K, & Pratap R, *Bioorg Med Chem*, 12 (2004) 883.
10 Liu M, Wilairat P, Croft S L, Tan A L C & Go M L, *Bioorg Med Chem*, 11 (2003) 2729.
11 Chen M, Christensen S B, Theander T G & Kharazmi A, *Antimicro Agents Chemo*, 38 (1994) 1339.
12 Troeberg L, Chen X, Flaherty T M, Morty R E, Cheng M, Hua H & Cohen F E, *Mol Med*, 6 (2000) 660.
13 Sarojini B K, Narayana B, Ashalatha B V, Indira J & Lobo K G, *J Cry Grow*, 295 (2006) 54.
14 Zhang Y, Guo Z & You X Z, *J Am Chem Soc*, 123 (2001) 9378.
15 Tanak H, Ağar A & Yavuz M, *J Mol Mod*, 16 (2010) 577.
16 Kurt M, Sertbakan T R & Özduran M, *Spectrochimica Acta A: Mol Biomol Spectro*, 70 (2008) 664.
17 Ravikumar C, Joe I H & Jayakumar V S, *Chem Phy Lett*, 460 (2008) 552.
18 Zhang R, Du B, Sun G & Sun Y, *Spectrochimica Acta A: Mol Biomol Spectro*, 75 (2010) 1115.
19 Verma A, Joshi S & Singh D, *J Chem*, 2013 (2013). (https://doi.org/10.1155/2013/329412)
20 Singhand H & Kapoor V K, *Medicinal and Pharmaceutical Chemistry*, 2nd ed., (Vallabh Prakashan, New Delhi) 2008.
21 Jin Z, *Nat Pro Rep*, 23 (2006) 464.
22 Molina P, Tárraga A & Otón F, *Org Biomol Chem*, 10 (2012) 1711.
23 Jin Z, Muscarine, *Nat Pro Rep*, 30 (2013) 869.
24 Vijesh A A, Isloor A M, Telkar S, Peethambar S K, Rai S & Isloor N, *Eur J Med Chem*, 46 (2011) 3531.
25 Kumar J R, *Hypertension*, 10 (2010) 11.
26 Frisch M J, Caricato M, Frisch A & Hiscocks J, Gaussian 09, Revision C, 2nd Ed., (Gaussian, Inc., Wallingford CT, USA) 2009.

27 Becke A D, *J Chem Phys*, 98 (1993) 5648.
28 Rauhut G & Pulay P, *J Phys Chem*, 99 (1995) 3093.
29 Dennington R I, Keith T, Millam J, Eppinnett K & Hovell W, *Gauss View Version 3.09*, 2003. (Kindly provide DOI number)
30 Mohanbabu B, Bharathikannan R & Siva G, *J Mat Sci Mat Elec*, 28 (2017) 1.
31 Koopmans T A, *Physica*, 1 (1993) 104
32 Chermette H, *J Comput Chem*, 20 (1999) 129.
33 Parr R G, Szentpaly L V & Liu S, *J Am Chem Soc*, 121 (1999) 1922.
34 Elleuch N, Amamou W, Ahmed A B, Abid Y & Feki H, J Spectrochem Acta A, 128 (2014) 781.
35 Das S J, Opt Mater, 29 (2007) 827.